Author/s:
Xu, X;Kentish, SE;Martin, GJO

Title:
Direct Air Capture of CO2by Microalgae with Buoyant Beads Encapsulating Carbonic Anhydrase

Date:
2021-07-26

Citation:
Xu, X., Kentish, S. E. & Martin, G. J. O. (2021). Direct Air Capture of CO2by Microalgae with Buoyant Beads Encapsulating Carbonic Anhydrase. ACS Sustainable Chemistry and Engineering, 9 (29), pp.9698-9706. https://doi.org/10.1021/acssuschemeng.1c01618.

Persistent Link:
https://hdl.handle.net/11343/281414

Direct air capture of CO_2 by microalgae with buoyant beads encapsulating carbonic anhydrase

Xiaoyin Xu † ‡, Sandra E. Kentish † * and Gregory J. O. Martin ‡

† Peter Cook Centre for CCS Research, Department of Chemical Engineering, The University of Melbourne, Parkville, Victoria 3010, Australia.

‡ Algal Processing Group, Department of Chemical Engineering, The University of Melbourne, Parkville, Victoria 3010, Australia

*Corresponding author email: sandraek@unimelb.edu.au

Abstract

Microalgae cultures have promise as a CO_2 sink for atmospheric carbon and as a sustainable source of food and chemical feedstocks. However, large-scale microalgae cultivation is currently limited by the need to provide carbon dioxide from point sources, as the diffusion of atmospheric CO_2 is too slow. Carbonic anhydrase (CA) is an effective enzyme to facilitate the dissolution of atmospheric CO_2 that could be used to enhance photosynthetic uptake of this greenhouse gas. Here we investigate a means of retaining CA at the surface of algae ponds to facilitate direct air capture by cross-linking CA with glutaraldehyde (GA) before encapsulation into buoyant calcium alginate beads. Coomassie Blue dyeing and Wilbur-Anderson assays confirmed the successful bonding of CA to the beads. Microscopic images showed the paraffin-embedded alginate framework. The CA-GA beads retain virtually all hydrase activity throughout 10 assay cycles. Compared with a natural growth rate of 22.7±0.5 mg L^{-1} d^{-1}, free CA and CA-GA beads increased the productivity of *Nannochloropsis salina* to 37±3 mg L^{-1} d^{-1} and 40±1 mg L^{-1} d^{-1}, respectively. The CA-GA beads further provided a stable growth enhancement for three rounds of microalgae cultivation, confirming that these buoyant beads can be readily recovered and re-used, which is promising for industrial biomass production.

Keywords: Carbonic anhydrase, CO_2 capture; calcium alginate; enzyme immobilization; *Nannochloropsis*

Introduction

Beyond simply curbing emissions, the removal of CO_2 from the atmosphere will be needed to mitigate the damaging effects of climate change. Direct-air capture of CO_2 is needed; however, this is a major challenge due to inherent limitations to the rate of CO_2 mass transfer and the need for a carbon sink. Only a small part of the CO_2 that must be captured can be utilized in industries such as enhanced oil recovery, food, and beverage production.[1] However, plants offer a means of converting atmospheric CO_2 into biomass. Biological utilisation of CO_2 via the production of terrestrial crops can also displace fossil-derived fuels and chemicals with alternatives produced from newly fixed carbon. However, conventional crop production is close to maximal, as evidenced by the food vs fuel issues arising from so-called 'first generation' biofuels produced from sugarcane and corn. Algae represent a promising alternative as they can grow at much higher productivities without the need for arable land and freshwater.[2] Industrial cultivation of microalgae can not only reduce CO_2 emissions but can also be used to remove nutrients in wastewater and to extract proteins and lipids as feedstocks for nutraceuticals, cosmetics, pharmaceuticals, or biofuels.[3-4]

One of the major limitations to mass production of algae is the provision of CO_2, which represents around 70% of the raw material costs in microalgae cultivation.[5] In addition, current production systems rely on a gaseous CO_2 source chemically captured and transported from large point sources, which limits the location of a microalgae plant to within the neighborhood of a CO_2 capture plant. Studies have investigated strategies to improve CO_2 delivery efficiency and decrease CO_2 cost, such as bubbling air mixed with a suitable portion of CO_2,[6-7] decreasing the size of gas bubbles to improve mass transfer,[8] and regulating bubbling rate by a pH monitor.[9] However, the high energy penalty of CO_2 capture, CO_2 compression, transport, and sparging is yet to be solved. In our previous work, a liquid-liquid membrane contactor was investigated to deliver dissolved CO_2 to the microalgae culture via semipermeable membranes.[10] Although this technique saved the energy cost of CO_2 compression and sparging, CO_2 was still required to be captured and transported from a capture plant.

A more abundant, sustainable and close CO_2 source is the atmosphere. However, the natural dissolution rate of atmospheric CO_2 is insufficient for the productive cultivation of densely grown algae. One option to overcome this slow uptake of CO_2 is the use of carbonic anhydrase (CA), a

group of enzymes able to rapidly catalyze the conversion of CO_2 to HCO_3^- (Eq. 1).[11] CA is widely present and accessible in living organisms including bacteria, archaea, algae and red blood cells. While CA has been widely studied in fields of CO_2 capture, CO_2 separation, biomedical and bioanalytical devices,[12-14] the application of CA in microalgae cultivation is quite limited. Hong et al.[15] prepared a CA-nanofiber composite which improved the productivity of *Dunaliella tertiolecta* by 80% when immersed in the culture medium and exposed only to atmospheric CO_2. This study showed the feasibility of CA-facilitated algae growth.

$$CO_2 + H_2O \overset{CA}{\leftrightarrow} HCO_3^- + H^+$$

Eq. 1

However, enzyme performance falls at a close distance from the reaction interface[16] due to the resistance to mass transfer of the gaseous CO_2 within the medium. Since CO_2 dissolution occurs at the air-culture interface, it is not cost-effective to disperse the relatively expensive CA, whether in its free or immobilized form, in the bulk culture. In addition, CA freely dissolved in an algae culture is susceptible to biodegradation by bacteria and proteolytic enzymes present.

To maximize the lifespan and effectiveness of the CA we propose a solution where immobilized CA is encapsulated within buoyant beads. Other researchers have similarly entrapped drugs inside excipients by emulsion-gelation methods for gastro-retentive drug delivery.[17-19] The excipient usually contains a polymer (e.g., alginate and pectinate) solution which forms a hydrogel when contacting with a cross-linker (typically, $CaCl_2$ solution). To make the bead float, either low-density substances (e.g., edible oils, magnesium stearate and gum) or gas-forming agents (e.g., bicarbonate and carbonate) can be added to the excipient.

For the reinforcement of enzyme immobilization, glutaraldehyde (GA) is commonly used as a crosslinking agent to form a covalent bond between the amino groups of the enzyme and the aldehyde group of the GA.[12, 15] For example, Tsai et al. aggregated β-Glucosidase by crosslinking with GA before entrapping inside a calcium alginate bead matrix.[20] This resulted in only 60% residual activity due to increased mass transfer resistance, but effectively avoided enzyme release and stabilized the enzyme activity throughout 20 rounds of reactions of 48 h each.

In this research, CA is cross-linked with GA and encapsulated in buoyant calcium alginate hydrogel beads to 1) retain CA at the air-culture interface where CA is most effective at capturing CO_2 directly from the atmosphere above, 2) improve the enzyme stability and prolong its

lifespan,[21] and 3) make it easier to recycle the enzyme. The enzyme activity and stability of both immobilized and free CA are compared. The glutaraldehyde cross-linking followed by alginate bead encapsulation is shown to be a suitable method to stabilize CA, being retained at the microalgae-atmosphere interface and enhancing the growth of microalgae.

Materials and Methods

Materials

CA derived from bovine erythrocyte, GA (25%), para-nitrophenyl acetate (p-NPA), para-nitrophenol (p-NP), thiamine hydrochloride, Nile red, fluorescein isothiocyanate (FITC), vitamin B_{12}, copper(II) sulfate pentahydrate ($CuSO_4 \cdot 5H_2O$), manganese(II) chloride tetrahydrate ($MnCl_2 \cdot 4H_2O$) and sodium molybdate dihydrate ($Na_2MoO_4 \cdot 2H_2O$) were purchased from Sigma-Aldrich (Castle Hill, Australia). Paraffin liquid, ferric citrate and selenous acid (H_2SeO_3) were obtained from Ajax Finechem (Sydney, Australia). Acetonitrile, citric acid, and potassium dihydrogen phosphate (KH_2PO_4) were from Merck (Kenilworth, United States). Tris(hydroxymethyl)aminomethane (Tris), sodium alginate, hydrochloric acid (HCl, 1N), sodium chloride ($CaCl_2$), zinc sulfate heptahydrate ($ZnSO_4 \cdot 7H_2O$), sodium nitrate ($NaNO_3$), and cobalt(II) chloride hexahydrate ($CoCl_2 \cdot 6H_2O$) were purchased from Chem-Supply (Gillman, Australia). All chemicals were used as purchased unless specifically mentioned. 50 mM Tris buffer was prepared with Tris and purified water (Millipore Elix) and adjusted to pH 8.0 by titrating with 1 N HCl.

As in previous work,[22] a marine strain of microalgae, *Nannochloropsis salina*, was obtained from the University of Melbourne Culture Collection. This species has been found to utilize HCO_3^- as a carbon source.[23] MF medium[24] was prepared as the algae culture medium by dissolving 33.4 g Red Sea Coral Pro Salt and 1 mL nutrient stock solution in 1 L purified water. The nutrient stock solution contained 200 g/L $NaNO_3$, 15.8 g/L KH_2PO_4, 9.0 g/L ferric citrate, 9.0 g/L citric acid, 6.4 mg/L $CuSO_4$, 12.9 mg/L $ZnSO_4$, 6.0 mg/L $CoCl_2$, 127 mg/L $MnCl_2$, 7.2 mg/L Na_2MoO_4, 0.65 mg/L H_2SeO_3, 0.5 mg/L vitamin B_{12}, 0.5 mg/L biotin and 100 mg/L thiamine hydrochloride.

CA Immobilization

The immobilization method (Figure S1) was modified from the literature.[17, 20] In brief, 5 mg CA,

5 mg GA, 0.5 mL 50 mM Tris buffer (pH 8.0), 0.12 g sodium alginate, and 0.5 g paraffin were mixed with purified water to 5g. Paraffin was selected as a density-modifying material since it has low density (0.86 g/mL), low volatility, is water-immiscible and not toxic to algae. The mixture was constantly stirred for 20 min until a homogeneous emulsion was formed. The emulsion was then extruded through a 25G needle (Terumo, Japan) at the rate of 0.3 mL/min by an NE-4000 syringe pump (Adelab Scientific, Australia) into a 5 % $CaCl_2$ solution. Beads containing CA formed as droplets of the emulsion interacted with the Ca^{2+}. The beads were taken out after 4 h and stored in Tris buffer at 4 ℃. The free CA concentration in the curing and storing solutions was measured by a Wilbur-Anderson assay (described below) to determine the CA loss during preparation and storage.

The size of 20 wet beads were measured by a digital micrometer (Mitutoyo, Japan) as 2.26±0.09 mm. The bead density was 0.91 g/mL, as calculated after measuring the weight and volume of 300 beads. The beads proved to maintain good buoyancy for a year.

Wilbur-Anderson activity assay (W-A assay)

The activity of CA is commonly evaluated by the W-A method.[25] In brief, 1.4 mL CA solution (or CA beads suspended in purified water) was mixed with 12.6 mL 50 mM Tris buffer in an ice bath before 6 mL of cold CO_2 saturated water was injected. A pH meter (S220 SevenCompact, Mettler Toledo, US) was used to monitor the pH and temperature of the mixture (around 4℃). A stopwatch was used to record the time. The Wilbur-Anderson Unit (WAU) is defined as (T_c/T_s)-1, where T_c and T_s refer to the time required for the pH to fall from 8.3 to 7.3 without and with the presence of CA respectively. Due to the slow speed of natural CO_2 hydration, T_c was measured every day when T_s was measured, and an average T_c was calculated as 270± 40 s based on 25 measurements. Sample dilution was used when the enzyme concentration was greater than 0.5 mg/L.

p-NPA activity assay

CA activity was also measured based on its esterase activity for hydrolysis of para-nitrophenyl acetate (p-NPA).[26] 100 μL of p-NPA in acetonitrile (2.5 mg/mL) was mixed with 4.9 mL of CA in Tris buffer immediately before the activity assay. The concentration of the 4-nitrophenol (p-NP) produced was quantified by a Cary 3E UV-Vis spectrophotometer (Varian, Palo Alto, US) at a wavelength of 348 nm, which is the isosbestic point of the products. The molar extinction

coefficient at 348nm was 5.2 mM^{-1} cm^{-1} according to calibration experiment completed by measuring the absorbance of p-NP solutions with the concentrations 0, 0.2, 0.4, 0.6 and 0.8 mM.

Coomassie Blue dyeing

Coomassie Brilliant Blue G-250 (CBBG) is a dye that can form non-covalent bonds with proteins.[27] It was thus used for enzyme identification in the alginate beads. CA-GA beads and blank beads were prepared in the same manner except for the addition or absence of CA. Two CA-GA beads and blank beads were suspended in 3 mL 0.01 mg/mL CBBG solution respectively. After storage under room temperature for 10 days, the light absorption of the solution was measured by a Cary 3E UV-Vis spectrophotometer (Varian, Palo Alto, US).

Microscopy

Wet beads were directly placed on a glass slide and observed under an OLYMPUS BX 51 Optical Microscope equipped with the software DP2 BSW.

The distribution of oil and protein in the beads was observed using a Nikon A1R+ Confocal Laser Scanning Microscope (CLSM, Tokyo, Japan) equipped with the software NIS-Elements AR. Before microscopy, the beads were stored in 50 mg/L FITC and 15mg/L Nile red solution overnight and rinsed with purified water. The beads were then placed on a glass slide. An air immersion 20× objective was used. Nile red and FITCs were imaged at excitation wavelengths of 488 nm and 561 nm respectively, and at emission wavelengths of 500-550 nm and 570-620 nm respectively. In the images acquired, FITC labelled-CA appeared green, Nile red-labelled paraffin appeared red and other phases appeared black.

For examination of the cross-section structure of the beads, they were frozen with liquid nitrogen and cut in half with a knife. The morphology was imaged by a scanning electron microscope (SEM) at an accelerating voltage of 15 kV (FlexSEM 1000, HITACHI, Tokyo, Japan). The microscope was equipped with a secondary electron (SE) detector, a back-scattered electron (BSE) detector, and an energy-dispersive X-ray (EDX) detector for element identification and mapping.

Algae cultivation

In most experiments, microalgae were grown in a 200 mL Schott bottle, magnetically stirred at 100 rpm. Since large-scale outdoor microalgae production is commonly performed in a raceway pond, a 10 L raceway pond detailed in our previous work[10] was also used as a further

demonstration. In both cases, the algae culture was diluted to 0.05 g/L with the MF medium at the start of each cultivation period. The algae were grown at room temperature (26±1 ℃) and illuminated by T5 Aquarium florescent globes from the top at 130±3 μmol m^{-2} s^{-1}. An AquaOne air pump was used to facilitate ventilation within the headspace of the bottles and raceway chambers, to ensure the replacement of CO_2-depleted air. Purified water was added on a daily basis to compensate for evaporation.

During microalgae growth, the culture pH and temperature were measured by the pH meter described above. Optical density (OD) was measured by the spectrophotometer at wavelength 750nm. OD can be converted to biomass concentration using the calibration formula: Biomass(g/L) = 0.2273OD (R^2=0.9992). Culture samples were filtered, acidified and the nitrate concentration measured based on the absorbance at 275nm and 220 nm (Ultraviolet Spectrophotometric Screening Method).[28] The total inorganic carbon (TIC) concentration was measured by a CM5015 CO_2 coulometer (UIC Inc., IL, US).

Results and Discussion

Characterization and biocatalytic application of free CA

To guide the subsequent immobilisation work, initial experiments were performed to assess the activity of different concentrations of free CA and their effect on the growth of *Nannochloropsis* sp. Figure 1(a) showed that the hydrase activity of free CA was linearly dependent on its concentration up to 0.4 mg/L. This trend did not continue at higher concentrations where the enzyme was more than needed. Within a 95% confidence level, the hydrase activity of CA was calculated to be 2800±300 WAU/mg CA, and the catalysed hydration rate was in the order of 10^5 mol CO_2 mol CA^{-1} s^{-1}, consistent with literature values 10^4 – 10^6 s^{-1}.[29] These results were used to quantify active CA concentration in a solution.

Similarly, p-NPA hydrolysis rate (Figure 1(b)) showed a distinct linear correlation to CA concentration. In contrast to the highly sensitive W-A assay, p-NPA assay featured a much wider optimal enzyme range which was 1-10 mg/L, allowing characterisation of enzyme activity beyond the linear range of the W-A method. Moreover, the catalysed hydrolysis rate was calculated as 0.14 mol p-NPA mol CA^{-1} s^{-1}, 10^6 times slower than the CO_2 hydration rate.

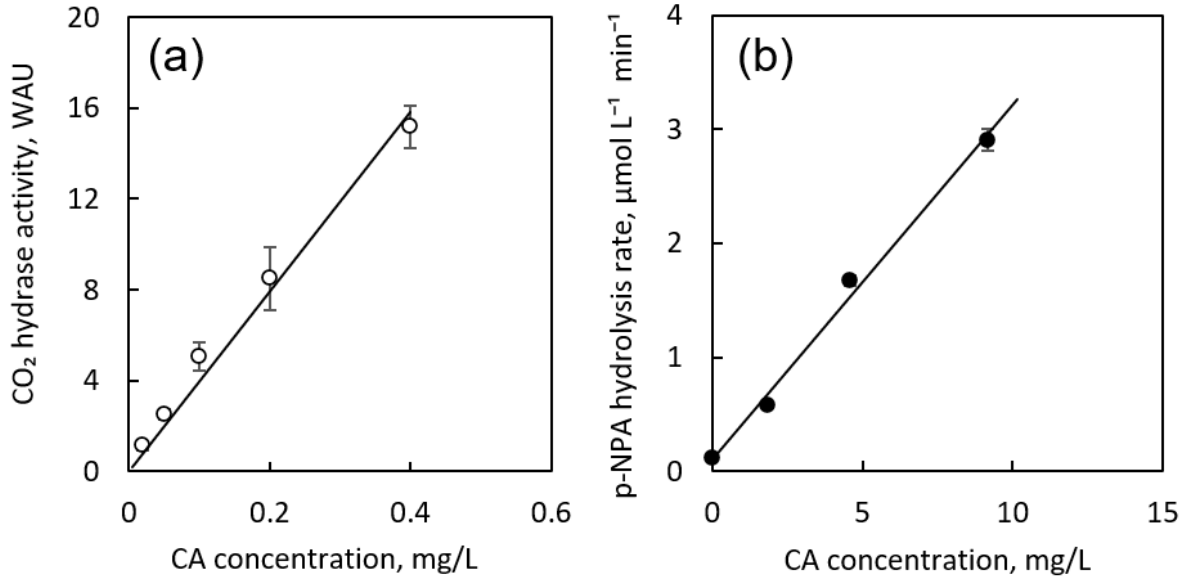

Figure 1 Correlation between free CA concentration and (a) CO_2 hydrase activity or (b) p-NPA esterase activity

Figure 2(a) shows the growth curves of *Nannochloropsis* sp. in MF medium with different free CA concentrations. Biomass accumulated steadily over time, while the growth rate increased with increasing CA concentration. This was due to the enrichment of inorganic carbon by CA activity. Typically, 40 mg/L of CA improved the growth of algae by 87%. However, supply and continual replacement of this amount of free CA is not economical, which emphasizes the importance of the surface immobilization technique.

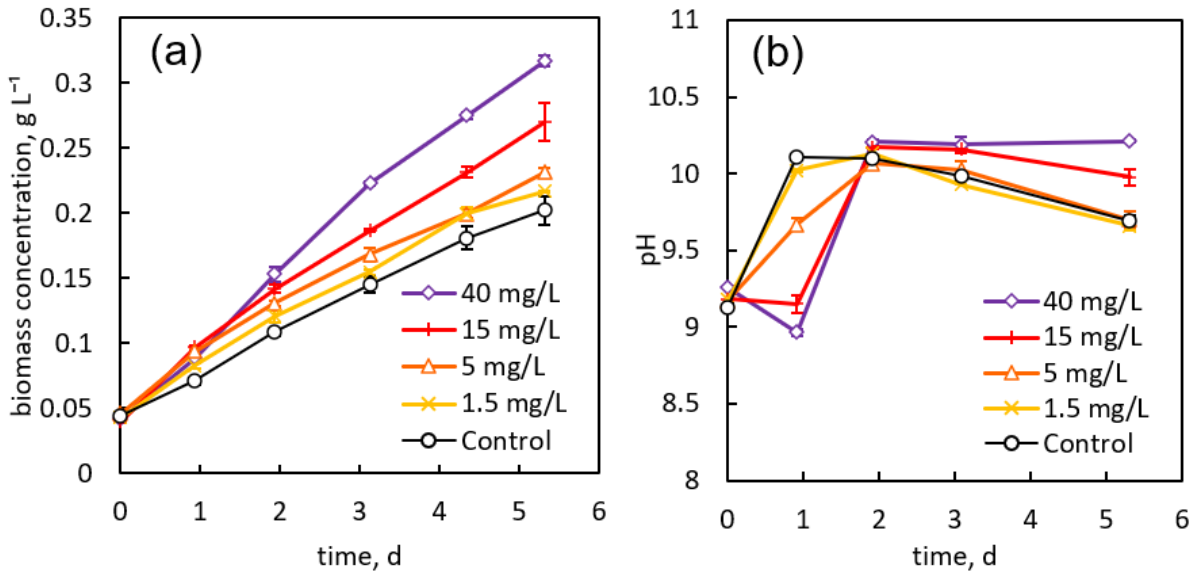

Figure 2 (a) Growth curves and (b) pH of *Nannochloropsis* sp. growing with different concentrations of free CA. Error bars represent the ranges of duplicate batches. The control is an identical culture without any CA addition.

A lower pH at higher CA concentration during the early days of growth (Figure 2(b)) is expected, as CO_2 hydration releases H^+. Interestingly, this trend is reversed after two days, probably because more algae cells utilized more HCO_3^- , thus absorbing H^+ for electric charge equilibrium. Another possible reason for the pH shift was that some enzyme degradation occurred. There have been reports that heavy metal cations and some anions can inhibit the activity of some CA enyzmes.[30-31] Since the algae grew in a marine environment with a range of ions, and the CA used was from a terrestrial source, the potential toxicity of the culture medium to CA cannot be discounted. Indeed, we observed a loss of CA activity via the W-A assay after four days when stored in seawater (Figure S2). However, immobilization of CA may reduce these effects.[32]

Development and characterization of buoyant CA beads

Various formulations for producing floating immobilized CA beads were investigated and the resulting beads characterized. In preliminary tests, the alginate concentration was found to be an important factor influencing the morphology of the CA beads. A higher concentration of alginate made the emulsion viscous and form a droplet-shaped hydrogel once pumped out through the needle tip (Figure S3); while a lower concentration of alginate was unable to fully crosslink with calcium ions to form a regular sphere shape. A similar trend has been found in previous research.[33]

Therefore, the final concentration of sodium alginate used in the following experiments was optimized to 2.4%.

Retention of the CA in the beads is critical during formulation and subsequent storage. Table 1 shows the CA loss during the preparation and storage process of CA and CA-GA beads. When the CA-containing emulsion droplet initially contacted the curing solution and Ca^{2+}-alginate cross-linking was not yet complete, loose CA enzyme was dispersed into the bulk solution readily, resulting in a CA loss as high as 88±3 %. The presence of GA dramatically reduced this value to 19±1 %, since the formation of GA-CA conjugates made them less likely to leach from the emulsion than free CA. CA loss during storage under quiescent conditions was much less significant. For both CA and CA-GA beads, the storing solution showed stable CA activity over a week, indicating no ongoing CA loss with time (data not shown), probably because a CA concentration equilibrium was reached between the bead surface and the storing solution.

Table 1 CA loss during the preparation and storage process

	CA loss in the curing solution	CA loss in the storing solution
CA beads	88±3 %	2.0±0.7 %
CA-GA beads	19±1 %	0.4±0.1 %

However, following repeated use, the hydrase activity of the CA beads without GA decreased significantly throughout cycles of the W-A assay, with only 16% left after 5 cycles (Figure 3), indicating further CA leaching from the beads in the washing step. Comparing the retention of CA during quiescent bead storage with the loss of CA during washing indicates loose entrapment of some of the enzyme. By contrast, when CA was cross-linked with GA before encapsulation, the beads retained around 100% activity throughout 10 assay cycles, which was attributed to a firm entrapment of the larger GA-CA conjugates inside the calcium alginate matrices. These results showed that the CA-GA beads had a higher resistance to enzyme leaching compared with CA beads. Therefore, later experiments were all performed with beads containing GA-CA aggregates.

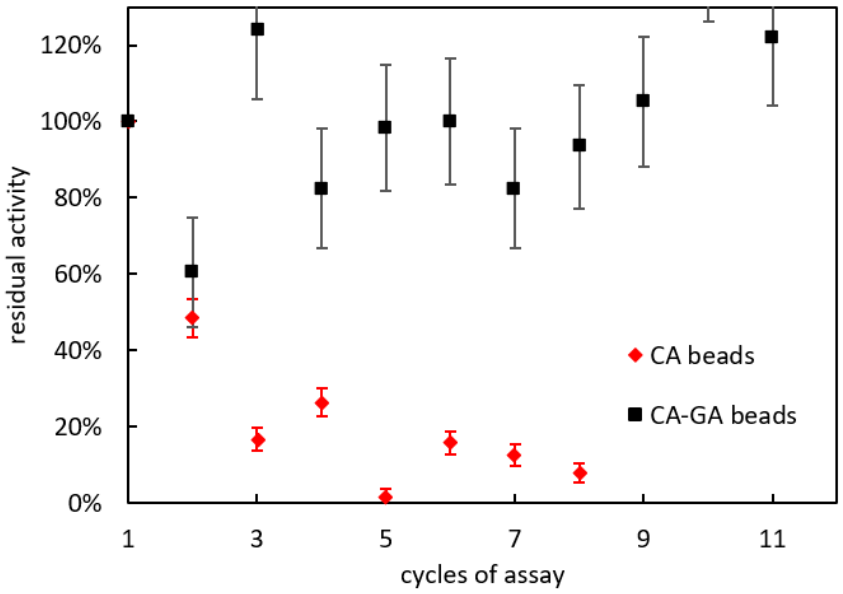

Figure 3 Residual activity of CA and CA-GA beads throughout repeated assays.

Further evidence of successful enzyme loading into the beads was given by CBBG dyeing. After incubating the colourless beads in the CBBG solution for 10d, both the CA-GA beads and blank beads were stained blue (Figure 4a). However, the CBBG concentration in the CA-GA bead vial, as given by the absorbance at 555nm, was only 34% of that in the blank bead vial (Figure 4b), indicating binding of the dye with protein (i.e. CA) contained within the beads.

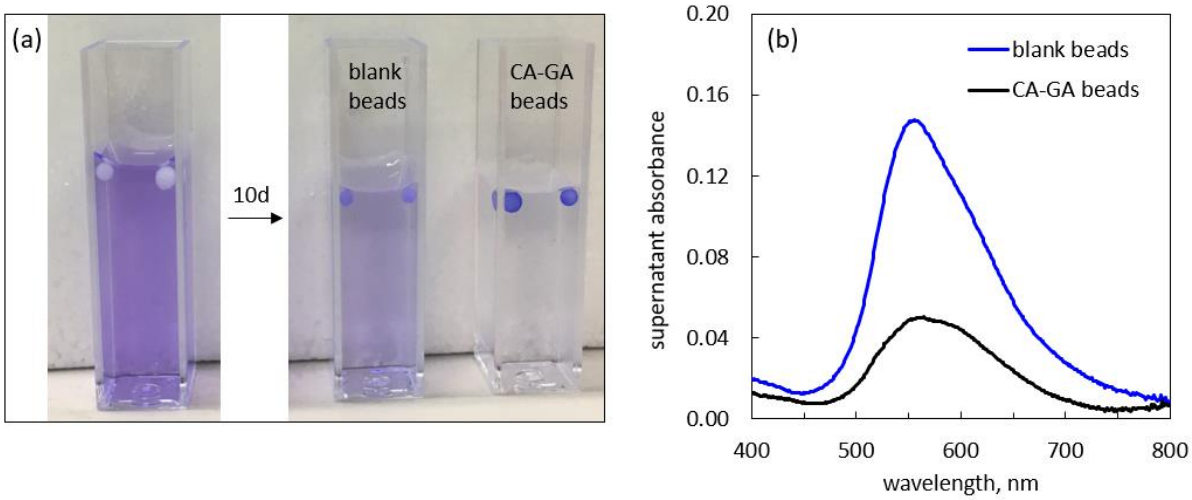

Figure 4 a) photos and b) absorption spectrum of a CBBG solution after incubating with CA-GA beads or blank beads for 10 d.

The microstructure and location of CA within the CA-GA beads were investigated by optical and confocal fluorescence microscopy (Figure 5). Under the optical microscope, the CA-GA beads were spherical (Figure 5a) with buoying droplets of paraffin visible beneath the exterior surface (Figure 5b). 100 droplets were captured from the image and the bead diameter was measured as 40±16 μm. The droplets within the beads, stained with Nile red, were confirmed as paraffin oil droplets (Figure 5d) under CLSM, while CA stained with FITC was found dispersed throughout the droplets (Figure 5c).

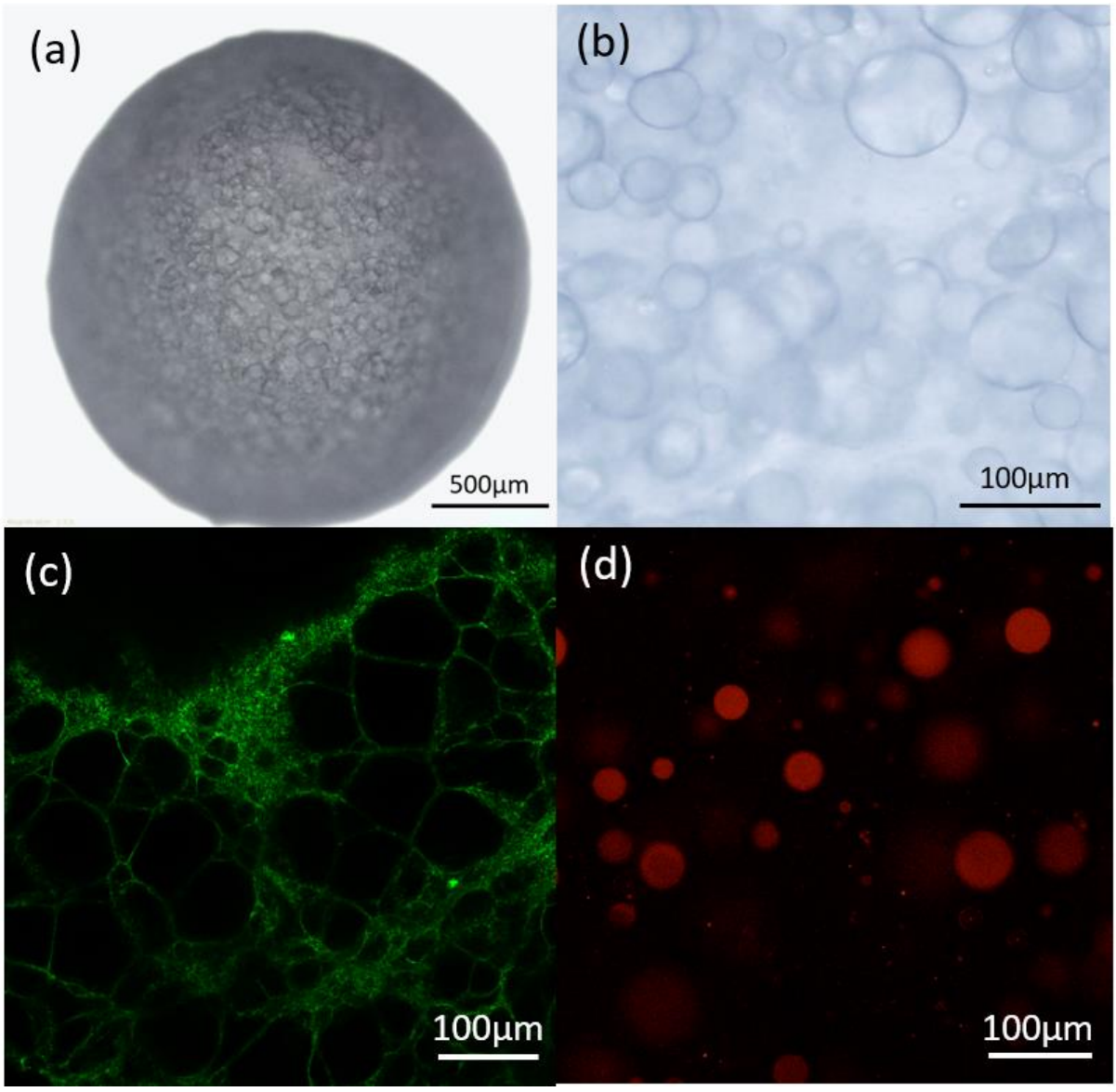

Figure 5 Microscopy images of the CA-GA beads: a-b) Optical microscopy images showing a whole bead and the interior of a bead; c-d) CLSM images. c) a dry bead, CA stained in green with FITC; d) a wet bead, paraffin stained in red with Nile red.

SEM images of the beads were also taken, showing the cross-section of the beads as a gelatinous texture with visible bulges dispersed (Figure 6a), consistent with the droplets observed beneath the surface (Figure 5a). Both BSE and EDX images (Figure 6b, c) provided information on atomic weight, where areas with heavier elements were brighter than those with lighter elements. As confirmation, element mapping showed a similar distribution of calcium (Figure 6e) to the bright area in Figure 6c. Oxygen atoms, mainly originated from alginate, were evenly distributed (Figure 6d). While carbon is expected in both paraffin and alginate phases, it was denser in paraffin droplets (Figure 6f) due to a higher carbon content (85 wt%). The map indicated that calcium alginate was evenly distributed as the framework of the beads, while paraffin droplets were successfully embedded to provide stable buoyancy.

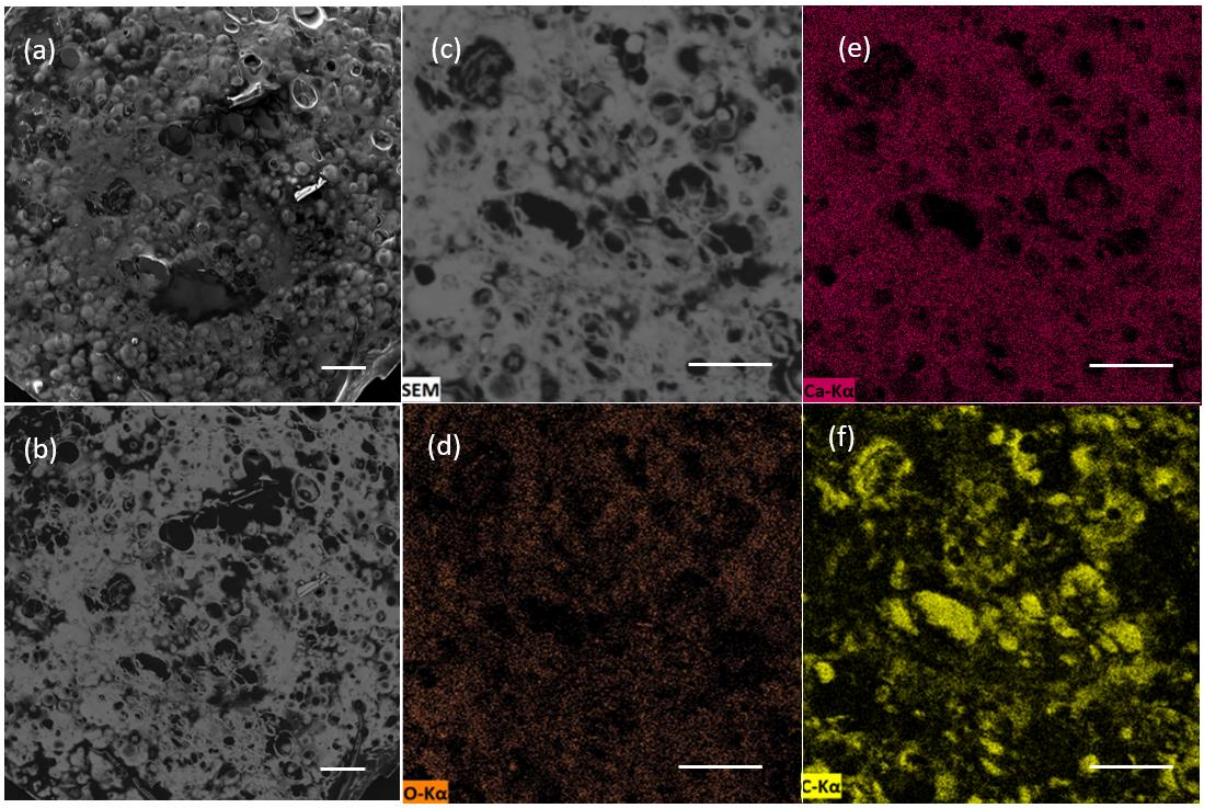

Figure 6 SEM images of a bead cross-section using a) secondary electron (SE) detector, b) back-scattered electron (BSE) detector and c-f) energy-dispersive X-ray (EDX) detector, showing element mapping of d) Oxygen e) Calcium f) Carbon. All scale bars represent 200μm.

CA-enhanced microalgae cultivation

Nannochloropsis sp. was cultivated under the following conditions: 1) a positive control group with air (0.04 vol% CO_2) sparging at a flow rate of 280 mL/min, providing more than sufficient

CO_2 to ensure light-limited growth; 2) a negative control group limited to absorbing CO_2 from the atmosphere representing carbon-limited growth; 3) with 2 g or 4 g of CA-GA beads facilitating CO_2 absorbance from the atmosphere; 4) free CA, with an equivalent mass of CA content as in 2 g of CA-GA beads, facilitating CO_2 absorbance from the atmosphere. In all the cases, CO_2 was utilized by algae via the pathway shown in Eq. 2. By consuming HCO_3^- via photosynthesis, the algae can maintain a concentration gradient of CO_2/ HCO_3^- to allow sustained uptake of CO_2 from the atmosphere. Biomass accumulated during the cultivation period (Figure 7a), and a higher growth rate also corresponds to more rapid consumption of nitrate (Figure 7b), which is a nutrient for the algae cells.

$$CO_2\ (\mathrm{g}) \overset{(1)}{\rightarrow} CO_2\ (\mathrm{aq}) \overset{(2)}{\rightarrow} HCO_3^- \rightarrow \textit{Nannochloropsis}\ \mathrm{sp.cell}$$

Eq. 2

Since CO_2 solubility in the water phase is low, the supply of atmospheric CO_2 is insufficient for concentrated algae growth in the natural environment, as was the case for the negative control group, which showed the lowest biomass growth rate 22.7±0.5 mg L^{-1} d^{-1} and nitrate consumption rate 1.38±0.03 mg L^{-1} d^{-1} (Figure 7). By contrast, air sparging marks the upper limit of the growth rate 100±3 mg L^{-1} d^{-1}, with the nitrate in the culture depleted in 4 days. Air bubbles increase the gas-liquid contacting area, generate turbulence and narrow the mass transfer boundary layer, thus accelerating the CO_2 dissolution reaction (Eq. 2, Step 1).

The presence of either free or immobilized CA enhanced algae growth to a similar extent: free CA improved the growth rate to 37±3 mg L^{-1} d^{-1}, while 2 g and 4 g of CA-GA beads achieved 40±1 mg L^{-1} d^{-1} and 43±1 mg L^{-1} d^{-1} respectively (Figure 7a). This was due to the use of CA accelerating the CO_2 hydration reaction (Eq. 2, Step 2). A similar growth enhancement for both 2 g and 4 g of CA-GA beads indicated that the CO_2 hydration reaction was "saturated" by the presence of the beads, for the gas-liquid surface area available. Thus, further reduction of the bead loading per unit surface area without compromising microalgal productivity is possible. Importantly, the use of immobilized CA-GA beads shows not only comparable algae growth enhancement factor to the free CA, but also a much greater potential for industrial implementation. After microalgae cultivation, the free CA cannot be recycled via centrifugation or filtration from the algal cells whose sizes lie in the range of micrometres. By contrast, the buoyant alginate CA-GA beads with diameters around 2 mm can either be retained during continuous cultivation and harvesting, or

skimmed directly from the culture surface for second-cycle re-use. This dramatically simplifies the separation process and increases their useful lifetime, therefore reducing the cost.

It should be mentioned that the apparent better performance of air sparging compared with CA-GA beads in the experiment is not expected to be retained at large-scale. Specifically, in a large-scale installation, sparging/agitation occurs at a single point of the pond. Conversely, the beads can be spread across the full pond area. Thus, the gas-liquid contacting area available in both approaches will ultimately be comparable, if not favour the beads. In a case study, it was shown that the air blower in a typical microalgae production plant that incorporates on-demand injection of pure CO_2 to maintain pH consumes 21% of the total energy, costing around 2.4USD/kg biomass.[5] With the use of CA-GA beads, this cost may be reduced dramatically by elimination or intermittent operation of the air blower.

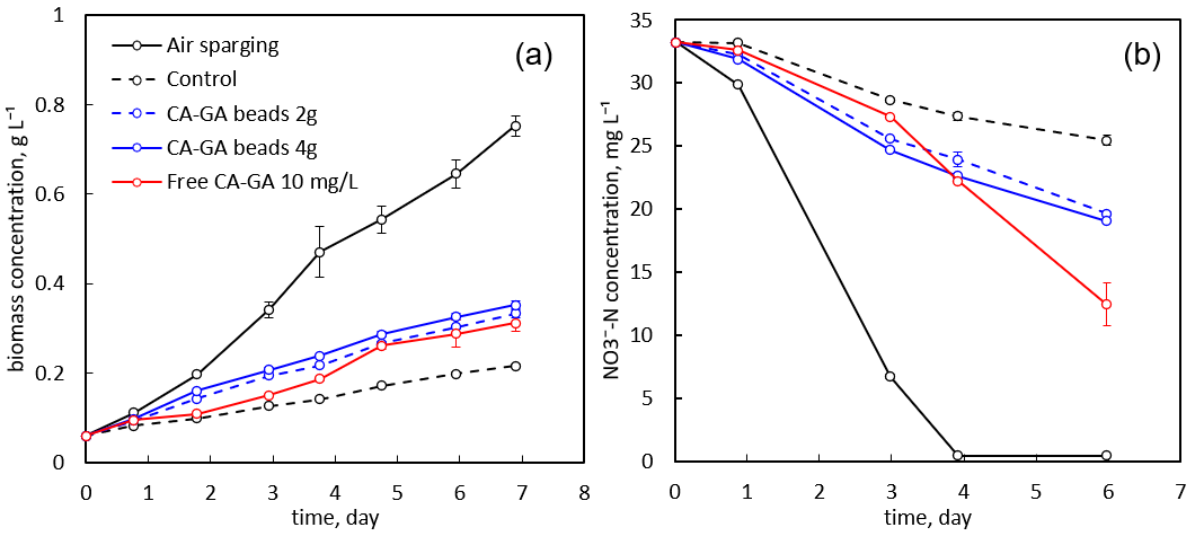

Figure 7 a) biomass and b) nitrate concentration in *Nannochloropsis* sp. cultures grown under different conditions as shown in the legend. Error bars represent the ranges of duplicate batches grown under identical conditions.

The total inorganic carbon (TIC) concentration in the culture of the control group decreased by 70% as the algae grew, indicating that the demand for CO_2/ HCO_3^- exceeded the supply (Figure 8). While the CA-GA beads did not provide a TIC concentration as high as freshly added (Day 1) free CA, the TIC concentration was more stable for the CA-GA beads, with 80% TIC remaining after 7 days. Given the algal growth was comparable for both cases, the higher TIC concentration may reflect less enzyme degradation with time.

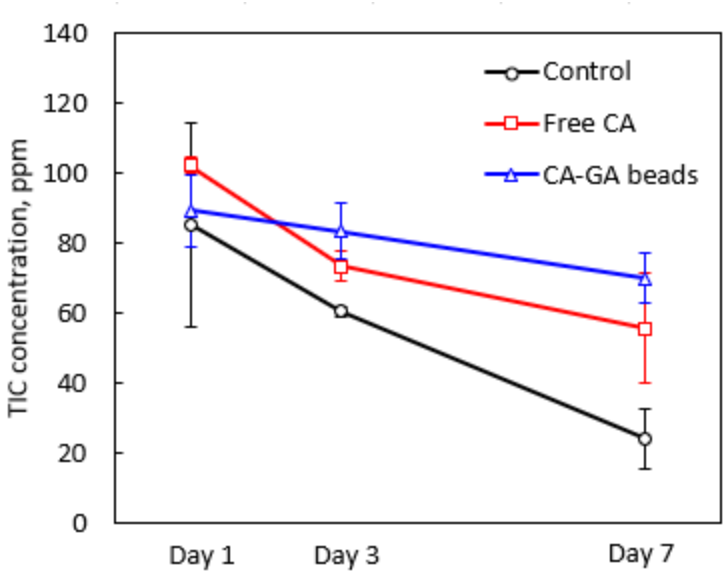

Figure 8 TIC concentration in the microalgae culture, for the control with no CO_2 addition, 2 g CA-GA of beads and the equivalent free CA group. Samples were taken on Days 1,3 and 7 of the cultivation period. Error bars represent the ranges of duplicate batches.

Fresh beads were repeatedly used in three rounds of 7-day cultivation of *Nannochloropsis* sp. The growth enhancement at this 7-day point was quite stable at around 40% (Figure 9a), proving the CA was stable when immobilized in the calcium alginate beads, compared to the poor stability of free CA in the marine medium (Figure S3). It was also found that water evaporation was slightly reduced (20% on average) due to the beads covering part of the culture surface (Figure 9b), which was beneficial for maintaining a stable culture environment. According to the measured bead density, 11% of the bead volume would be exposed to the air, and the theoretical surface coverage of 2g beads to the algae culture was thus estimated as 33%. However, the water loss of only 20% indicated that around 1/3 of the beads were being temporarily immersed in the medium by the vortex of the stirrer. This problem can be readily avoided at a large-scale algal pond with a calmer water surface, which promises a higher growth enhancement factor for the beads.

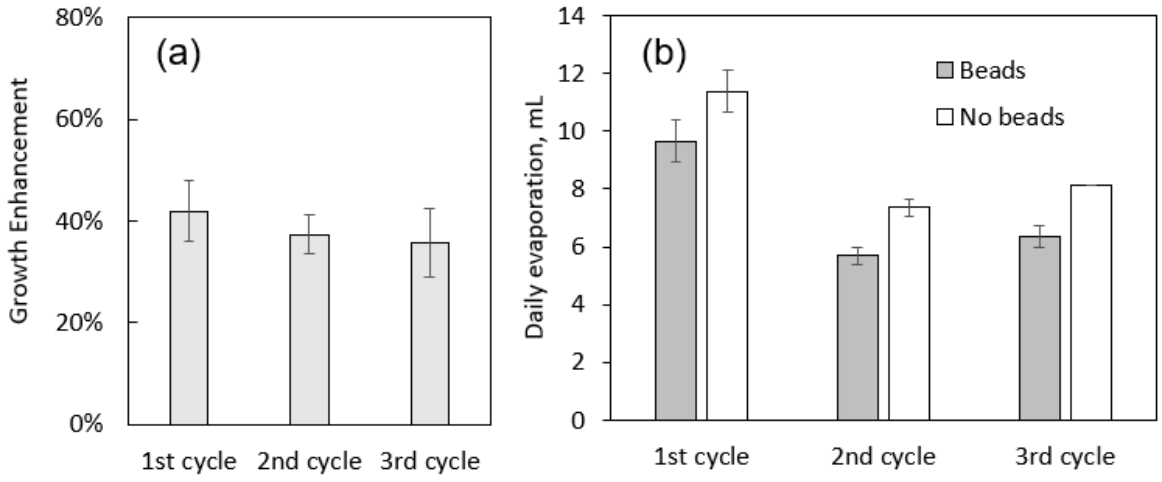

Figure 9 a) Growth enhancement and b) water evaporation of 200 mL *Nannochloropsis* sp. culture grown with 2g CA-GA beads in three cycles. Error bars represent the ranges of duplicate batches.

In the mini raceway pond (Figure 10a), the growth of *Nannochloropsis* sp. was again improved upon the addition of these beads, to 4.4±0.1 g m^{-2} d^{-1}, corresponding to a CO_2 fixation rate of 8.0±0.2 g m^{-2} d^{-1} (Figure 10b). According to this result, a typical 100 m^2 raceway pond is able to purify (2.22±0.06) $\times 10^4$ m^3 air per day by reducing the CO_2 concentration by 20 ppm. The growth enhancement in the raceways was 16%, compared to 75% in the smaller scale set up (Figure 7a). Similar to the previous discussion about air sparging, this was possibly because the paddle wheel, which is disproportionately large compared to the paddle wheel in a full-scale algal pond, provides significant aeration (and CO_2 delivery) to the control group. Also, many of the beads became attached to the stirrer blades over the growth period and did not float freely, which is a problem that could be easily avoided or managed on a large scale (in which the paddle wheels occupy a much smaller proportion of the raceways).

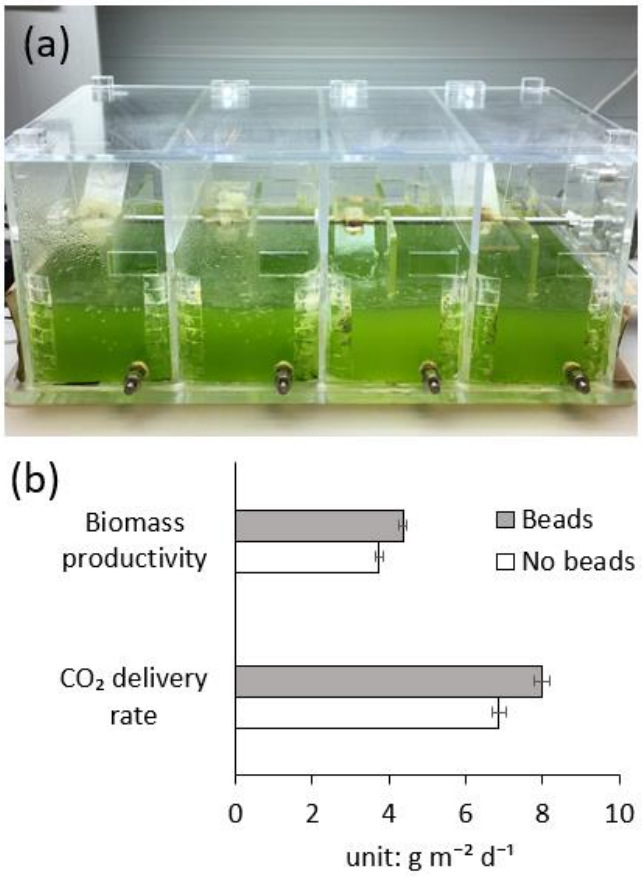

Figure 10 a) Nannochloropsis sp. growing in a mini raceway pond with CA-GA beads (left two chambers) and without CA-GA beads (right two chambers) and b) growth parameters of *Nannochloropsis* sp. growing in a mini raceway pond with and without CA-GA beads.

Based on the CA-catalysed CO_2 hydration rate measured in the W-A assay, 1 cm^2 of the bead surface area exhibited a CO_2 hydration rate of 5.2 µmol min^{-1}. Assuming the carbon content is 50% of the dry cell mass, to achieve a target microalgae biomass productivity of 25 g m^{-2} d^{-1} in a traditional raceway pond, 5.0 g beads are needed per square metre of algae culture, corresponding to only 0.35% of the pond surface coverage, which is low enough to ignore the side effect of light shadowing. At lab-scale, CA accounts for over 98% of the material costs of bead production. Based on the previous assumptions, Table 2 outlines some projected cost scenarios as a function of scale and CA lifetime. Assuming a CA lifetime of a fortnight as a conservative estimate, the lab-scale cost for the beads is around $46 per tonne of dry biomass. However, a greater number of lifecycles can be possible, particularly if a CA enzyme can be developed that is more resistant to seawater and other impurities (e.g., if a CA from a marine microalga could be produced at scale); or if a freshwater algae species is used. Further, the cost of the enzyme itself is expected to reduce

significantly if produced on a large scale by using genetically modified bacteria, lowering the requirement for extensive purification, and increasing the production volume and fermentation yield.[34] The price of industrially produced crude isolated CA can be reduced by orders of magnitude to \$0.3-3.0/g.[35-36] Under these conditions, the cost of CA-GA beads is thus projected to fall, possibly to around \$0.02 per tonne of dry biomass.

Table 2 Estimated cost of CA-GA beads needed to produce algal biomass in different scenarios, in USD per tonne of dry biomass.

CA lifetime, d	Laboratory scale†	Industrial scale‡
2	325	0.89
14	46	0.13
100	6.5	0.02

Note: † Assuming CA is purchased from the supplier Sigma-Aldrich with a price of \$1822/g.

‡ Assuming CA is produced economically at a large scale with the price of \$5/g.

Importantly, this approach allows for the direct air capture of carbon dioxide, while simultaneously providing an opportunity to remove waste nutrients from wastewater and to produce valuable biomass. Compared to direct air capture, where the energy penalty is around USD\$3.65 GJ/t CO_2[37], the energy demand here is only that required to harvest and process the algal products. Similarly, the cost for direct air capture is currently predicted to be between USD\$270[38] and 1300[37] while in the present case, biodiesel can be produced with a price of between USD\$0.5 and 2 per kg alongside other potentially even more valuable products such as protein, pigments and lipids[39-41], with the potential to thus render the approach cost neutral.

Conclusions

In this work, we have demonstrated a CA immobilization technique, where CA is cross-linked with GA before encapsulation into buoyant calcium alginate beads, facilitating their placement at the air-medium boundary. Two CA activity assay methods were compared and their calibration curves for CA quantification were established. CA bonding to the beads was confirmed by CBBG dyeing and W-A assays. GA proved a good cross-linker to retain CA within the beads, reducing CA loss in the bead formation process by 62%. The residual activity of the CA-GA beads was almost 100% after 10 assay cycles. Both free CA and CA-GA beads improved microalgae growth,

but the CA-GA beads were able to maintain a stable TIC content, stable growth enhancement factor and a reduction in water evaporation. The cost of the beads is expected to reduce to US$0.02/t biomass on a large scale with a prolonged lifespan. Given the stability, recyclability and low cost, CA-GA beads are promising for improving large-scale microalgae production and direct air capture of CO_2.

Acknowledgements

This work was generously supported by the Pratten Foundation. Funding was also provided by the Australian Research Council (ARC) through the Discovery Projects Grant Scheme (DP200101230). The authors would also like to acknowledge the Particulate Fluids Processing Centre and the Peter Cook Centre at the University of Melbourne for access to instruments. Xiaoyin Xu is grateful to the University of Melbourne for providing a Melbourne Research Scholarship.

Supporting Information

Figure S1 Workflow of the preparation of buoyant beads.

Figure S2 Residual activity of free CA stored in in Tris buffer and seawater over time at room temperature.

Figure S3 Morphology of calcium alginate hydrogels with different alginate contents in the emulsion.

References

1. Brinckerhoff, P., Accelerating the uptake of CCS: industrial use of captured carbon dioxide. *Global CCS Institute* **2011**, 260.

2. Ahmad, A. L.; Yasin, N. H. M.; Derek, C. J. C.; Lim, J. K., Microalgae as a sustainable energy source for biodiesel production: A review. *Renewable and Sustainable Energy Reviews* **2011,** *15* (1), 584-593. https://doi.org/10.1016/j.rser.2010.09.018.

3. Raeesossadati, M. J.; Ahmadzadeh, H.; McHenry, M. P.; Moheimani, N. R., CO2 bioremediation by microalgae in photobioreactors: Impacts of biomass and CO2 concentrations, light, and temperature. *Algal Research* **2014,** *6* (Part A), 78-85. https://doi.org/10.1016/j.algal.2014.09.007.

4. Judd, S.; van den Broeke, L. J. P.; Shurair, M.; Kuti, Y.; Znad, H., Algal remediation of CO2 and nutrient discharges: A review. *Water Research* **2015,** *87*, 356-366. https://doi.org/10.1016/j.watres.2015.08.021.
5. Acién, F. G.; Fernández, J. M.; Magán, J. J.; Molina, E., Production cost of a real microalgae production plant and strategies to reduce it. *Biotechnology Advances* **2012,** *30* (6), 1344-1353. https://doi.org/10.1016/j.biotechadv.2012.02.005.
6. Assunção, J.; Batista, A. P.; Manoel, J.; da Silva, T. L.; Marques, P.; Reis, A.; Gouveia, L., CO2 utilization in the production of biomass and biocompounds by three different microalgae. *Eng. Life Sci.* **2017,** *17* (10), 1126-1135. https://doi.org/10.1002/elsc.201700075.
7. Mortezaeikia, V.; Tavakoli, O.; Yegani, R.; Faramarzi, M., Cyanobacterial CO2 biofixation in batch and semi-continuous cultivation, using hydrophobic and hydrophilic hollow fiber membrane photobioreactors. *Greenhouse Gases: Science and Technology* **2016,** *6* (2), 218-231. https://doi.org/10.1002/ghg.1542.
8. Zimmerman, W. B.; Tesař, V.; Bandulasena, H. C. H., Towards energy efficient nanobubble generation with fluidic oscillation. *Current Opinion in Colloid & Interface Science* **2011,** *16* (4), 350-356. https://doi.org/10.1016/j.cocis.2011.01.010.
9. Jiang, Y.; Zhang, W.; Wang, J.; Chen, Y.; Shen, S.; Liu, T., Utilization of simulated flue gas for cultivation of Scenedesmus dimorphus. *Bioresource Technology* **2013,** *128*, 359-364. https://doi.org/10.1016/j.biortech.2012.10.119.
10. Xu, X.; Martin, G. J. O.; Kentish, S. E., Enhanced CO2 bio-utilization with a liquid–liquid membrane contactor in a bench-scale microalgae raceway pond. *Journal of CO2 Utilization* **2019,** *34*, 207-214. https://doi.org/10.1016/j.jcou.2019.06.008.
11. Zheng, Q.; Xu, X.; Martin, G. J. O.; Kentish, S. E., Critical review of strategies for CO2 delivery to large-scale microalgae cultures. *Chinese Journal of Chemical Engineering* **2018,** *26*, 2219-2228. https://doi.org/10.1016/j.cjche.2018.07.013.
12. Yoshimoto, M.; Walde, P., Immobilized carbonic anhydrase: preparation, characteristics and biotechnological applications. *World Journal of Microbiology and Biotechnology* **2018,** *34* (10), 151. https://doi.org/10.1007/s11274-018-2536-2.
13. Hu, G.; Smith, K. H.; Nicholas, N. J.; Yong, J.; Kentish, S. E.; Stevens, G. W., Enzymatic carbon dioxide capture using a thermally stable carbonic anhydrase as a promoter in potassium carbonate solvents. *Chemical Engineering Journal* **2017,** *307*, 49-55. https://doi.org/10.1016/j.cej.2016.08.064.
14. Zhang, Y.-T.; Zhang, L.; Chen, H.-L.; Zhang, H.-M., Selective separation of low concentration CO2 using hydrogel immobilized CA enzyme based hollow fiber membrane reactors. *Chemical Engineering Science* **2010,** *65* (10), 3199-3207. https://doi.org/10.1016/j.ces.2010.02.010.
15. Hong, S.-G.; Jeon, H.; Kim, H. S.; Jun, S.-H.; Jin, E.; Kim, J., One-Pot Enzymatic Conversion of Carbon Dioxide and Utilization for Improved Microbial Growth. *Environmental Science & Technology* **2015,** *49* (7), 4466-4472. https://doi.org/10.1021/es505143f.
16. Penders-van Elk, N. J. M. C.; Hamborg, E.; Huttenhuis, P. J. G.; Fradette, S.; Carley, J.; Versteeg, G. F., Kinetics of absorption of carbon dioxide in aqueous amine and carbonate solutions with carbonic anhydrase. *International journal of greenhouse gas control* **2013,** *12*, 259-268. https://doi.org/10.1016/j.ijggc.2012.10.016.
17. Sriamornsak, P.; Thirawong, N.; Puttipipatkhachorn, S., Morphology and buoyancy of oil-entrapped calcium pectinate gel beads. *The AAPS Journal* **2004,** *6* (3), 65-71. https://doi.org/10.1208/aapsj060324.
18. Malakar, J.; Nayak, A. K., Formulation and statistical optimization of multiple-unit ibuprofen-loaded buoyant system using 23-factorial design. *Chemical Engineering Research and Design* **2012,** *90* (11), 1834-1846. https://doi.org/10.1016/j.cherd.2012.02.010.

19. Bera, H.; Boddupalli, S.; Nandikonda, S.; Kumar, S.; Nayak, A. K., Alginate gel-coated oil-entrapped alginate–tamarind gum–magnesium stearate buoyant beads of risperidone. *International journal of biological macromolecules* **2015,** *78*, 102-111. https://doi.org/10.1016/j.ijbiomac.2015.04.001.
20. Tsai, C.-T.; Meyer, A., Enzymatic cellulose hydrolysis: enzyme reusability and visualization of β-glucosidase immobilized in calcium alginate. *Molecules* **2014,** *19* (12), 19390-19406. https://doi.org/10.3390/molecules191219390.
21. Zhang, Y.-T.; Zhi, T.-T.; Zhang, L.; Huang, H.; Chen, H.-L., *Immobilization of carbonic anhydrase by embedding and covalent coupling into nanocomposite hydrogel containing hydrotalcite*. 2009; Vol. 50, p 5693-5700.
22. Olmstead, I. L. D.; Hill, D. R. A.; Dias, D. A.; Jayasinghe, N. S.; Callahan, D. L.; Kentish, S. E.; Scales, P. J.; Martin, G. J. O., A quantitative analysis of microalgal lipids for optimization of biodiesel and omega-3 production. *Biotechnology and Bioengineering* **2013,** *110* (8), 2096-2104. https://doi.org/doi:10.1002/bit.24844.
23. Mustaffa, N. I. H.; Striebel, M.; Wurl, O., Extracellular carbonic anhydrase: Method development and its application to natural seawater. *Limnology and Oceanography: Methods* **2017,** *15* (5), 503-517. https://doi.org/10.1002/lom3.10182.
24. Guillard, R. R.; Ryther, J. H., Studies of marine planktonic diatoms: I. Cyclotella nana Hustedt, and Detonula confervacea (Cleve) Gran. *Canadian journal of microbiology* **1962,** *8* (2), 229-239. https://doi.org/10.1139/m62-029.
25. Wilbur, K. M.; Anderson, N. G., Electrometric and colorimetric determination of carbonic anhydrase. *Journal of biological chemistry* **1948,** *176* (1), 147-154. https://doi.org/10.1016/S0021-9258(18)51011-5.
26. Yong, J. K. J.; Cui, J.; Cho, K. L.; Stevens, G. W.; Caruso, F.; Kentish, S. E., Surface Engineering of Polypropylene Membranes with Carbonic Anhydrase-Loaded Mesoporous Silica Nanoparticles for Improved Carbon Dioxide Hydration. *Langmuir* **2015,** *31* (22), 6211-6219. https://doi.org/10.1021/acs.langmuir.5b01020.
27. Cao, Y.; Zhao, J.; Xiong, Y. L., Coomassie Brilliant Blue-binding: a simple and effective method for the determination of water-insoluble protein surface hydrophobicity. *Analytical methods* **2016,** *8* (4), 790-795. https://doi.org/10.1039/C5AY02630J.
28. Standard Methods for the Examination of Water and Wastewater. American Public Health Association: Washington, DC, USA, 2005.
29. Dodgson, S. J., The carbonic anhydrases. In *The carbonic anhydrases*, Springer: 1991; pp 49-70.
30. Li, L.; Fu, M.-l.; Zhao, Y.-h.; Zhu, Y.-t., Characterization of carbonic anhydrase II from Chlorella vulgaris in bio-CO2 capture. *Environ. Sci. Pollut. Res.* **2012,** *19* (9), 4227-4232. https://doi.org/10.1007/s11356-012-1077-8.
31. Pocker, Y.; Stone, J. T., The Catalytic Versatility of Erythrocyte Carbonic Anhydrase. III. Kinetic Studies of the Enzyme-Catalyzed Hydrolysis of p-Nitrophenyl Acetate*. *Biochemistry* **1967,** *6* (3), 668-678. https://doi.org/10.1021/bi00855a005.
32. Mateo, C.; Palomo, J. M.; Fernandez-Lorente, G.; Guisan, J. M.; Fernandez-Lafuente, R., Improvement of enzyme activity, stability and selectivity via immobilization techniques. *Enzyme and Microbial Technology* **2007,** *40* (6), 1451-1463. https://doi.org/10.1016/j.enzmictec.2007.01.018.
33. Li, Z. Q.; Hou, L. D.; Li, Z.; Zheng, W.; Li, L. In *Study on shape optimization of calcium–alginate beads*, Advanced Materials Research, Trans Tech Publ: 2013; pp 125-130.
34. Molina-Fernández, C.; Luis, P., Immobilization of carbonic anhydrase for CO2capture and its industrial implementation: A review. *Journal of CO2 Utilization* **2021,** *47*, https://doi.org/10.1016/j.jcou.2021.101475.

35. Tufvesson; Tufvesson, P. r.; Lima Ramos, J.; Nordblad, M.; Woodley, J. M., Guidelines and Cost Analysis for Catalyst Production in Biocatalytic Processes. *Organic Process Research & Development* **2011,** *15* (1), 266-274. https://doi.org/10.1021/op1002165.
36. Gilassi; Gilassi, S.; Taghavi, S.; Rodrigue, D.; Kaliaguine, S., Techno-economic evaluation of membrane and enzymatic-absorption processes for CO2 capture from flue-gas. *Separation and purification technology* **2020,** *248*, 116941. https://doi.org/10.1016/j.seppur.2020.116941.
37. Krekel, D.; Samsun, R. C.; Peters, R.; Stolten, D., The separation of CO2 from ambient air – A techno-economic assessment. *Applied Energy* **2018,** *218*, 361-381. https://doi.org/10.1016/j.apenergy.2018.02.144.
38. Fasihi, M.; Efimova, O.; Breyer, C., Techno-economic assessment of CO2 direct air capture plants. *Journal of Cleaner Production* **2019,** *224*, 957-980. https://doi.org/10.1016/j.jclepro.2019.03.086.
39. Gebreslassie, B. H.; Waymire, R.; You, F., Sustainable design and synthesis of algae-based biorefinery for simultaneous hydrocarbon biofuel production and carbon sequestration. *AIChE Journal* **2013,** *59* (5), 1599-1621. https://doi.org/10.1002/aic.14075.
40. Gong, J.; You, F., Value-Added Chemicals from Microalgae: Greener, More Economical, or Both? *ACS Sustainable Chemistry & Engineering* **2015,** *3* (1), 82-96. 10.1021/sc500683w.
41. García Prieto, C. V.; Ramos, F. D.; Estrada, V.; Villar, M. A.; Diaz, M. S., Optimization of an integrated algae-based biorefinery for the production of biodiesel, astaxanthin and PHB. *Energy* **2017,** *139*, 1159-1172. https://doi.org/10.1016/j.energy.2017.08.036.

Abstract Graphic

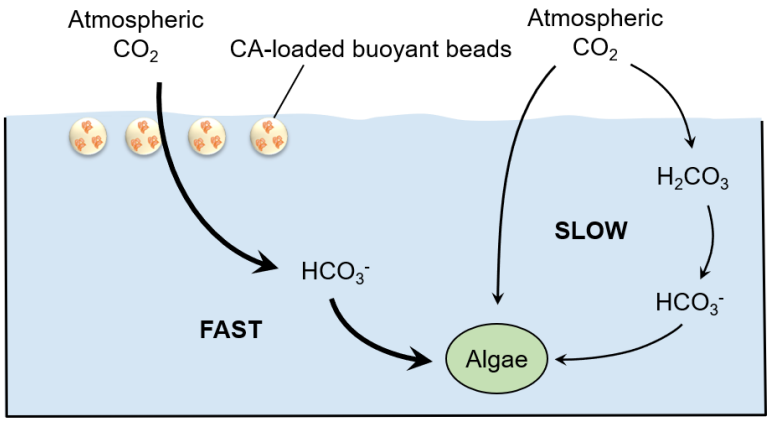

Synopsis

Carbonic anhydrase facilitates the direct air capture of CO_2 to drive industrial cultivation of microalgae, by placement at the gas-liquid interface within buoyant beads.